Published in final edited form as:
Cancer Res. 2012 May 1; 72(9): 2285–2293. doi:10.1158/0008-5472.CAN-11-3836.

Hypoxia-inducible factor-2α activation promotes colorectal cancer progression by dysregulating iron homeostasis

Xiang Xue[1], **Matthew Taylor**[1], **Erik Anderson**[1], **Cathy Hao**[1], **Aijuan Qu**[4], **Joel K. Greenson**[3], **Ellen M. Zimmermann**[2], **Frank J. Gonzalez**[4], and **Yatrik M. Shah**[1,2,*]

[1]Department of Molecular & Integrative Physiology, University of Michigan, Ann Arbor, MI.

[2]Department of Internal Medicine, Division of Gastroenterology, University of Michigan, Ann Arbor, MI.

[3]Department of Pathology, University of Michigan, Ann Arbor, MI.

[4]Laboratory of Metabolism, Center for Cancer Research, National Cancer Institute, National Institutes of Health, Bethesda, MD.

Abstract

Hypoxia-inducible factor (HIF), a key modulator of the transcriptional response to hypoxia, is increased in colon cancer. However, the role of HIF in colon carcinogenesis in vivo remains unclear. In this study, we found that intestinal epithelium-specific disruption of the von Hippel-Lindau tumor suppressor protein (VHL) resulted in constitutive HIF signaling, and increased HIF expression augmented colon tumorigenesis in the *Apc*$^{min/+}$ intestinal tumor model. Intestine-specific disruption of Vhl increased colon tumor multiplicity and progression from adenomas to carcinomas. These effects were ameliorated in mice with double disruption of Vhl and HIF-2α. Activation of HIF signaling resulted in increased cell survival in normal colon tissue, however tumor apoptosis was not affected. Interestingly, a robust activation of cyclin D1 was observed in tumors of *Apc*$^{min/+}$ mice in which HIF-2α was activated in the intestine. Consistent with this result, BrdU incorporation indicated that cellular proliferation was increased in colon tumors following HIF activation. Further analysis demonstrated that dysregulation of the intestinal iron absorption transporter divalent metal transporter-1 (DMT-1) was a critical event in HIF-2α-mediated colon carcinogenesis. These data provide a mechanistic basis for the widely reported link between iron accumulation and colon cancer risk. Together, our findings demonstrate that a chronic increase in HIF-2α in the colon initiates pro-tumorigenic signaling which may have important implications in developing preventive and therapeutic strategies for colon cancer.

Keywords

hypoxia-inducible factor-2α; colon cancer; *Apc*$^{min/+}$; iron homeostasis; divalent metal transporter-1

Introduction

Hypoxic microenvironment is a hallmark for solid tumors (1). In response to hypoxia, tumor cells activate genes that are critical in angiogenesis, cell survival, cell proliferation, and

*Correspondence: Yatrik M. Shah, Department of Molecular & Integrative Physiology, Department of Internal Medicine Division of Gastroenterology, University of Michigan, Ann Arbor, MI. shahy@umich.edu.

Disclosure of Potential Conflicts of Interest: No potential conflicts of interest were disclosed.

glucose metabolism(2). Hypoxia-induced signal transduction is transcriptionally mediated by hypoxia-inducible factor (HIF), a member of the Per-ARNT-Sim family of basic helix-loop-helix transcription factors that bind hypoxia response elements (HREs) at target gene loci under hypoxic conditions(3–5). Functional HIF is a heterodimer that comprises a constitutive subunit, aryl hydrocarbon nuclear translocator (Arnt, also known as HIF-1β) and a hypoxia-inducible alpha subunit(3, 4). Stabilization of the α-subunit is regulated by a family of oxygen and iron-dependent prolyl hydroxylase (PHD) enzymes. PHD enzymes hydroxylate the α-subunit enabling the binding of the von Hippel-Lindau tumor suppressor protein (VHL) coupled to the E3 ubiquitin ligase complex, which leads to proteasomal degradation of HIF-α subunits(6, 7).

Two highly homologous and transcriptionally active subunits have been identified, HIF-1α and HIF-2α(8, 9). Both are expressed in many of the same cells and regulate overlapping and distinct sets of genes critical in the adaptation to hypoxic environments, including cancer development(10). In cancer-derived cell lines and in renal carcinomas, HIF-1α and HIF-2α have opposing roles in cell proliferation. HIF-1α decreases cell proliferation whereas HIF-2α induces proliferation via an increase in c-Myc activity(11–16). HIF-1α and HIF-2α are overexpressed in a variety of tumor tissues including colon cancer(17, 18). However, the role of HIF-α in colon carcinogenesis is not completely clear.

The present study demonstrates that $Apc^{min/+}$ mice with an intestine-specific activation of HIF signaling via disruption of *Vhl* using a villin-cre recombinase developed mainly colorectal tumors, with carcinomas seen in 8 of 10 (80%) mice followed for 6 months. Disruption of both *Vhl* and *Hif-2α* in intestinal epithelial cells prevented colon tumors indicating a HIF-2α-dependent mechanism. Through global gene expression analysis in the $Apc^{min/+}$ mice and human colorectal tumor samples, a HIF-2α-dependent dysregulation of colon iron homeostasis was observed. Increase in local iron levels have been implicated in the progression colon carcinogenesis (19–25), and the present data demonstrate the increase in tumor iron exacerbated cell proliferation and was critical in colon tumor formation following HIF-2α activation. Together, these data reveal a novel role for HIF-2α in initiating a coordinated process that is critical in the progression of colon cancer.

Materials and Methods

Animals and diets

The floxed or compound floxed mice hemizygous for villin-cre were mated to each other to generate $Vhl^{F/F}$, $Vhl^{\Delta IE}$, $Vhl^{F/F}/Hif\text{-}2\alpha^{F/F}$, $Vhl^{\Delta IE}/Hif\text{-}2\alpha^{\Delta IE}$ mice and are described previously(26–28). $Apc^{min/+}$ were purchased from The Jackson Laboratory. To investigate the role of HIF-2α in colorectal cancer, $Vhl^{\Delta IE}$ and $Vhl^{\Delta IE}/Hif\text{-}2\alpha^{\Delta IE}$ mice were crossed with $Apc^{min/+}$ mice to generate $Vhl^{F/F}/Apc^{min/+}$, $Vhl^{\Delta IE}/Apc^{min/+}$, $Vhl^{\Delta IE}/Hif\text{-}2\alpha^{\Delta IE}/Apc^{min/+}$, and $Vhl^{F/F}/Hif\text{-}2\alpha^{F/F}/Apc^{min/+}$ mice. All mice were 129S6/SvEv background and maintained in standard cages in a light and temperature-controlled room and were allowed standard chow and water *ad libitum*. For low-iron study, the 6-week-old $Vhl^{\Delta IE}/Apc^{min/+}$ and $Vhl^{F/F}/Apc^{min/+}$ mice were given iron-replete AIN93G diet containing 350 ppm of iron or iron-deficient AIN93G diet (less than 5 ppm of iron) for 8-weeks (Dyets, Bethlehem, PA). All animal studies were carried out in accordance with Institute of Laboratory Animal Resources guidelines and approved by the University Committee on the Use and Care of Animals at the University of Michigan (UCUCA approval number: 10299).

Histology, immunohistochemistry, and immunofluorescence

For BrdU staining, animals were sacrificed following a 2-hour treatment of 100 mg/kg of BrdU (Sigma, St Louis, MO). Paraffin-embedded tissue sections (5-μm) were deparaffinized

in xylene, and rehydrated in ethanol gradient. Immunohistochemical analysis was performed with antibodies for BrdU (Bu20a, eBioscience Inc., San Diego, CA) followed by detection using Alexa Fluor® 488 goat anti-mouse IgG (Molecular Probes Inc., Eugene, OR). TUNEL assay (Roche Diagnostics, Indianapolis, IN) was performed according to the supplier's instructions. Briefly, deparaffinized sections were labeled with TdT and biotinylated dUTP, and then were examined under a fluorescence microscope (29). Tissue iron detection was performed in paraffin embedded sections stained with Perls Prussian blue and enhanced with DAB and H_2O_2 (30). Histological analysis was done on hematoxylin and eosin stained paraffin sections and microscopically analyzed by a gastrointestinal pathologist.

Quantitative Real-Time RT-PCR (qPCR)

RNA was isolated from fresh or frozen tissue using Isol-RNA lysis reagent (3 Prime, Gaithersburg, MD). After quantification with NanoDrop 2000 (NanoDrop products, Wilmington, DE), RNA with a purity of ~ 2.0 (260/280 ratio) was reverse-transcribed using M-MLV Reverse Transcriptase (Fisher Scientific, Waltham, MD). cDNA was quantified using SYBR green dye and run on a 7900HT Fast Real Time RT-PCR system (Life Technologies, Carlsbad, CA) (primers listed in Supplemental Table 1). Ct values were normalized to β-actin and expressed as fold difference from controls.

Western blot analysis

Tissues were homogenized and lysed in radioimmunoprecipitation assay (RIPA) buffer (50 mM Tris-HCl pH 7.5, 150 mM NaCl, 2 mM EDTA, 1% NP-40, 0.1% SDS) for whole cell extracts. Proteins were separated and transferred to nitrocellulose membranes using standard methods. Membranes were incubated with antibodies against cleaved keratin 18 (K18) (kindly provided by Prof. Bishr Omary, University of Michigan), total caspase 3, cleaved caspase 3 (Cell Signaling Technology Inc., Beverly, MA), HIF-2α (Novus Biologicals, Littleton, CO), DMT-1 (alpha Diagonostic, San Antonio, TX) and GAPDH (Santa Cruz Biotechnology, Santa Cruz, CA) followed by incubation with appropriate HRP-conjugated secondary antibodies (Cell Signaling Technology Inc.). Blots were detected using the Enhanced Chemiluminescence Detection kit (Thermo Scientific, Wayne, MI).

Primary colon organoid and other cell culture

For organoid whole-colon cultures, colons were opened longitudinally and were rinsed gently and quickly placed in culture medium, RPMI-1640 plus 10% heat inactivated fetal bovine serum (FBS) and 1% antibiotic/antimycotic (1 units/mL of penicillin, 1 μg/mL of streptomycin, and 2.5ng/mL of amphotericin B) (Life Technologies, Carlsbad, CA). The colons were cut into 5- to 7-mm pieces and incubated in the culture medium described above for 2-hour at 37 °C, 5% CO_2/21% O_2. After incubation, tissues were homogenized and lysed in RIPA buffer to perform Western blot analysis as described above. HCT116 cells were obtained from ATCC and maintained at 37 °C in 5% CO_2 and 21% O_2. Cells were cultured in DMEM supplemented with 10% FBS and 1% antibiotic/antimycotic. Early passaged (P10) stable HIF-2α and parental HCT116 cells were generated by transfection of a normoxically stable HIF-2α or pIRES puro 3 empty vector with lipofectamine 2000 (Life Technologies) according to manufacturer's instructions and selected by 2 μg/mL puromycin. The cells were maintained in growth media described above containing 1 μg/mL of puromycin.

PolyHema Apoptosis Assay

Cell adhesion to proper extracelluar matrix is essential for epithelial cell survival. Failure of attachment leads to a form of apoptosis termed anoikis (31). Poly-hydroxyl-ethyl-meth-acrylate (PolyHema) is a polymer which can form a surface that prevents cell adherence

when coated on cell culture plate(32). Twenty-four well plates were coated with 250 μL/well PolyHema (20 mg/mL) to achieve nonadherent conditions. HIF-2α overexpressing or parental HCT116 cells were plated at a concentration of 1×10^4 cells/mL in DMEM supplemented with 10% FBS and 1% antibiotic/antimycotic into PolyHema coated plates or non-coated control plates. After 24- or 48-hour culture, 125 μL 5 mg/mL Thiazolyl Blue Tetrazolium Bromide (MTT) (Sigma) reagent was added to each well and incubated for 30 minutes. DMSO was added and absorbance was measured at 570 nm.

cDNA microarray analysis

RNA was extracted from colon mucosal scrapings from 5 weeks old *Vhl*$^{F/F}$, *Vhl*$^{\Delta IE}$, *Vhl*$^{F/F}$/*Apc*$^{min/+}$ and *Vhl*$^{\Delta IE}$/*Apc*$^{min/+}$ mice. Isolated RNA with RNA integrity number values >6.5 examined by Agilent 2100 bioanalyzer (Agilent Technologies, Inc., Santa Clara CA) was amplified, reverse transcribed, labeled, and hybridized to mouse 430 2.0 Affymetrix GeneChips (Affymetrix, Santa Clara, CA), and data were analyzed as previously described(28). The full data set is available on the GEO database accession number GSE36091.

Statistics

Results are expressed as mean ± S.D. P values were calculated by independent t-test, One-way ANOVA, Dunnett's t-test, and two-way ANOVA. $p<0.05$ was considered significant.

Results

Activation of HIF-2α potentiates colon carcinogenesis following APC mutation

Mice with an intestine-specific disruption of *Vhl* (*Vhl*$^{\Delta IE}$) activate HIF signaling, whereas no induction of HIF signaling is observed in littermate controls (*Vhl*$^{F/F}$)(28, 33). To assess the role of HIF in intestinal tumorigenesis, these mice were crossed to the *Apc*$^{min/+}$ mice (Supplemental Figure 1A). *Apc*$^{min/+}$ mice have a nonsense mutation at codon 850 of the murine *Apc* gene leading to a truncated protein (34). Adenomatous polyposis coli (APC) is a tumor suppressor protein highly relevant in colon cancer; over 80% of patients with sporadic colon cancer have a somatic mutation of the *Apc* gene(35), and mutations are observed in early and late colitis associated neoplasms(36–38). In patients with *Apc* mutations, the predominant cancer is colon cancer and very rarely (≈10 fold less) are small intestinal tumors observed(39). However, *Apc*$^{min/+}$ mice develop mostly small intestinal tumors(34). Consistent with previous data, *Vhl*$^{F/F}$/*Apc*$^{min/+}$ mice developed predominantly small intestinal tumors. In the small intestine, tumors were found in 17/17 3-month-old *Vhl*$^{F/F}$/*Apc*$^{min/+}$ mice, with a tumor multiplicity of 32.24, whereas 4/17 *Vhl*$^{F/F}$/*Apc*$^{min/+}$ mice developed tumors in the colon with a tumor multiplicity of 0.59. Interestingly, *Vhl*$^{\Delta IE}$ mice crossed to the *Apc*$^{min/+}$ background had a dramatic shift in the tumor localization to the colon in 3-month-old mice (Figure 1A–1C). Small intestinal tumors were significantly decreased in the 3-month-old *Vhl*$^{\Delta IE}$/*Apc*$^{min/+}$ compared to *Vhl*$^{F/F}$/*Apc*$^{min/+}$ mice (tumor incidence: 11/15 mice; tumor multiplicity: 2.80). However, a significant increase in tumor incidence and numbers were observed in the colon of 3-month-old *Vhl*$^{\Delta IE}$/*Apc*$^{min/+}$ mice (tumor incidence: 15/15 mice; tumor multiplicity: 13.87). Consistent with this, Western blotting analysis demonstrated an increase of HIF-2α protein expression in both normal colon and tumor tissues from *Vhl*$^{\Delta IE}$/*Apc*$^{min/+}$ mice (Supplemental Figure 2). To assess whether the changes in tumor number and incidence were dependent on HIF-2α, a double knockout mouse model of *Vhl* and *Hif-2α* on an *Apc*$^{min/+}$ background (*Vhl*$^{\Delta IE}$/*Hif-2α*$^{\Delta IE}$/*Apc*$^{min/+}$) was generated and compared to littermate controls (*Vhl*$^{F/F}$/*Hif-2α*$^{F/F}$/*Apc*$^{min/+}$) (Supplemental Figure 1B). Interestingly, small intestinal tumors in *Vhl*$^{\Delta IE}$/*Hif-2α*$^{\Delta IE}$/*Apc*$^{min/+}$ mice were significantly repressed compared to the *Vhl*$^{F/F}$/*Hif-2α*$^{F/F}$/*Apc*$^{min/+}$ mice. These data were similar to that observed in the *Vhl*$^{\Delta IE}$/*Apc*$^{min/+}$ mice indicating that

VHL-mediated decrease in small intestinal tumorigenesis is independent of HIF-2α (Figure 1B and 1C). However, the increase in the colon tumorigenesis in $Vhl^{\Delta IE}/Apc^{min/+}$ mice was completely ablated following compound knockout of *Vhl* and *Hif-2α* in the $Apc^{min/+}$ background, demonstrating that HIF-2α plays a critical role in the development of colon cancer (Figure 1B and 1C). These results were further confirmed in the 6-month-old $Vhl^{\Delta IE}/Apc^{min/+}$ and $Vhl^{\Delta IE}//Hif\text{-}2\alpha^{\Delta IE}/Apc^{min/+}$ mice (Figure 1D and 1E). Compared to 3-month-old $Vhl^{F/F}/Apc^{min/+}$ mice, the tumor multiplicities in 6-month-old $Vhl^{F/F}/Apc^{min/+}$ mice were increased in the small intestine (tumor multiplicity: 62.50, tumor incidence: 6/6 mice) and colon (tumor multiplicity: 1.33, tumor incidence: 3/6 mice). However, small intestinal tumors were still significantly decreased in the 6-month-old $Vhl^{\Delta IE}/Apc^{min/+}$ (tumor incidence: 10/10 mice; tumor multiplicity: 15.10) compared to 6-month-old $Vhl^{F/F}/Apc^{min/+}$ mice. The tumor incidence and numbers observed in the colon of 6-month-old $Vhl^{\Delta IE}/Apc^{min/+}$ mice (tumor incidence: 10/10 mice; tumor multiplicity: 14.50) were not further increased compared to 3-month-old $Vhl^{\Delta IE}/Apc^{min/+}$ mice. However, they were still significantly increased compared to 6-month-old $Vhl^{F/F}/Apc^{min/+}$ mice. Assessing the double knockout mice ($Vhl^{\Delta IE}/Hif\text{-}2\alpha^{\Delta IE}/Apc^{min/+}$) at 6-months further demonstrated that the decrease in small intestinal tumorigenesis is independent of HIF-2α, whereas the increase in colon carcinogenesis is completely dependent on HIF-2α.

Activation of HIF-2α increases tumor progression in the $Apc^{min/+}$ mice

All tumors assessed in the small intestine or colon from 3- and 6-month-old $Vhl^{F/F}/Apc^{min/+}$ mice demonstrated well-organized glandular structures and were classified as adenomas (Figure 2A). However, 2 out of 15 tumors from 3-month-old $Vhl^{\Delta IE}/Apc^{min/+}$ mice demonstrated early signs of carcinoma formation (Figure 2B and 2D). In 6-month-old $Vhl^{\Delta IE}/Apc^{min/+}$ mice, 8 out of 10 mice had colon tumors that displayed complex glands with cribriform architecture and desmoplastic stroma, and thus were classified as carcinomas (Figure 2C and 2D). To assess if the increase in colon cancer progression was HIF-2α-dependent, tumor analysis was performed on 6-month-old $Vhl^{\Delta IE}/Hif\text{-}2\alpha^{\Delta IE}/Apc^{min/+}$ mice (Figure 2D). Although adenomas were observed, no tumors progressed to carcinomas. These data demonstrate that activation of HIF-2α is critical for the progression of colon tumors.

HIF-2α regulates cell survival in the colon

Analysis of apoptosis in colon tumors between $Vhl^{F/F}/Apc^{min/+}$ and $Vhl^{\Delta IE}/Apc^{min/+}$ was performed using TUNEL assay. No significant difference was observed in tumors from $Vhl^{F/F}/Apc^{min/+}$ and $Vhl^{\Delta IE}/Apc^{min/+}$ mice (Supplemental Figure 3). Interestingly, a dramatic increase in cell survival was observed in normal colon epithelial cells of $Vhl^{\Delta IE}$ mice compared to $Vhl^{F/F}$ mice. Intestinal epithelial cells undergo a spontaneous form of apoptosis termed anoikis as the differentiated cells reach the villus tips and are shed(40). Capturing this by TUNEL or caspase staining is difficult. Therefore, the apoptotic response of primary colon organoids generated from $Vhl^{F/F}$ and $Vhl^{\Delta IE}$ mice were compared. The colons from $Vhl^{F/F}$ and $Vhl^{\Delta IE}$ mice were isolated and snap frozen immediately or cultured for 2-hour. Upon culturing, the colon undergoes a dramatic induction of anoikis-induced apoptosis as seen with increased expressions of cleaved keratin 18 and cleaved caspase 3 in colons isolated from $Vhl^{F/F}$ mice (Figure 3A). However, in colons cultured from $Vhl^{\Delta IE}$ mice, significant decreases in cleaved keratin 18 and cleaved caspase 3 expressions were observed (Figure 3A). In contrast, cleaved keratin 18 and cleaved caspase 3 expressions were partially restored in colons cultured from $Vhl^{\Delta IE}/Hif\text{-}2\alpha^{\Delta IE}$ mice (Figure 3A). To further confirm these results, a stable HIF-2α overexpressing colon-derived HCT116 cell line was generated. As expected, in parental HCT116 cells, HIF-2α was not detectable whereas in the stable overexpressing cells, a dramatic increase in HIF-2α expression was observed (Figure 3B). Cell survival was assessed in an anoikis-induced apoptotic assay.

Cells were incubated in poly-hema coated plates to inhibit attachment, leading to increased apoptosis. Parental cells demonstrated decreased survival rate following 24- and 48-hour of incubation. The survival rate was significantly increased in HCT116 cells overexpressing HIF-2α (Figure 3C) with a concordant decrease in the activation of caspase 3 following 24-hour of incubation on poly-hema coated plates (Figure 3D). Although no significant difference is observed in tumor apoptosis (Supplemental Figure 3), activation of HIF-2α induces cell survival that may play an important role in colon tumor progression.

HIF-2α regulates cell proliferation in colon cancer

Since apoptosis could not fully explain the increase in colon tumor formation in the $Vhl^{\Delta IE}/Apc^{min/+}$ mice, the contribution of cell proliferation to HIF-2α induced colon cancer was assessed. Cyclin D1 expression was assessed in $Vhl^{\Delta IE}/Apc^{min/+}$ and $Vhl^{F/F}/Apc^{min/+}$ mice by qPCR analysis. No significant difference of cyclin D1 expression was observed in the normal colon tissues of $Vhl^{F/F}/Apc^{min/+}$ and $Vhl^{\Delta IE}/Apc^{min/+}$ mice. However, cyclin D1 was significantly induced in the colon tumors of $Vhl^{\Delta IE}/Apc^{min/+}$ mice compared to tumors isolated from $Vhl^{F/F}/Apc^{min/+}$ mice (Figure 4A). Consistent with cyclin D1 expression, BrdU incorporation revealed no significant difference in the normal colon tissues of $Vhl^{F/F}/Apc^{min/+}$ and $Vhl^{\Delta IE}/Apc^{min/+}$ mice (Figure 4B and C). However, the numbers of BrdU positive proliferating epithelial cells in the colon tumors of $Vhl^{\Delta IE}/Apc^{min/+}$ mice were significantly higher than those in tumors of $Vhl^{F/F}/Apc^{min/+}$ mice (Figure 4B and 4C). Elevated tumor proliferation was ablated in the colon tumors of $Vhl^{\Delta IE}/Hif\text{-}2\alpha^{\Delta IE}/Apc^{min/+}$ mice (Figure 4D). These data demonstrate that HIF-2α increases tumor cell proliferation, which may be critical for the increase in colon tumor formation and progression.

Divalent metal transporter-1 (DMT-1) and iron uptake represent a cellular target and regulator of HIF-2α-induced colon cancer

To identify the precise molecular mechanisms that could contribute to the increase in colon carcinogenesis, microarray gene expression analysis was performed on colon RNA isolated from 5-week-old $Vhl^{F/F}$ and $Vhl^{\Delta IE}$, $Vhl^{\Delta IE}/Apc^{min/+}$ and $Vhl^{F/F}/Apc^{min/+}$ mice. The data identified 469 genes that were significantly increased/decreased in both $Vhl^{\Delta IE}$ and $Vhl^{\Delta IE}/Apc^{min/+}$ compared to their littermate controls and 29 genes that were significantly increased/decreased in both $Vhl^{F/F}/Apc^{min/+}$ and $Vhl^{\Delta IE}/Apc^{min/+}$ compared to their littermate *Apc* wild-type controls (Figure 5A). The top ten genes that were regulated in a HIF-2α-dependent manner were further assessed utilizing ONCOMINE (Supplemental Table 2), a cancer microarray data-mining platform(41). Those genes that were increased in the colons of $Vhl^{\Delta IE}/Apc^{min/+}$ mice and in human colon cancer samples were identified. This analysis demonstrated a specific increase in DMT-1 expression in colon adenomas and carcinomas isolated from patients compared to normal controls in 3 independent studies(42–44) (Figure 5B). DMT-1 is the major apical iron transporter in the intestine(45–47). It is essential for iron absorption and its expression in the small intestine is directly regulated by HIF-2α(26). Colon tumors have been shown to accumulate iron(23). Moreover, mouse models of colon cancer and population-based studies demonstrate a direct correlation between an increase in intestinal iron and increased incidence of colon cancer(24, 25). These studies suggest that dysregulation of local iron homeostasis is critical in colon carcinogenesis. Consistent with these results, measuring tissue iron using enhanced Prussian iron staining demonstrated a significant increase in iron accumulation in colon tumors compared to normal tissue (Figure 5C). To assess whether HIF-2α was critical for DMT-1 regulation during colon tumorigenesis, DMT-1 expression was measured by qPCR. DMT-1 was significantly induced in the colons of $Vhl^{F/F}/Apc^{min/+}$ mice compared to wild-type littermates ($Vhl^{F/F}$), which was further potentiated in $Vhl^{\Delta IE}/Apc^{min/+}$ mice compared to wild-type littermates in a HIF-2α-dependent manner (Figure 5D). Similar expression patterns were also noted in the small intestine (Supplemental Figure 4). Western blotting

analysis further demonstrated that DMT-1 protein expression was increased in a HIF-2α-dependent manner in colon tumors (Figure 5E).

Low-iron treatment reduces HIF-2α-induced colon tumor formation

To verify that the increase in iron contributed to the increase in colon carcinogenesis, $Vhl^{\Delta IE}/Apc^{min/+}$ and $Vhl^{F/F}/Apc^{min/+}$ mice were placed on control or low-iron diet. As expected, the $Vhl^{\Delta IE}/Apc^{min/+}$ mice on control diet demonstrated increased colon tumor numbers compared to littermate controls (Figure 6A). The increase in colon tumors was completely ablated in $Vhl^{\Delta IE}/Apc^{min/+}$ mice on low-iron diet for 2 months (Figure 6A). Analysis of BrdU incorporation revealed no significant difference in the normal colon tissues of $Vhl^{F/F}/Apc^{min/+}$ and $Vhl^{\Delta IE}/Apc^{min/+}$ mice treated with control diet. The number of BrdU positive proliferating epithelial cells in the colon tumors of $Vhl^{\Delta IE}/Apc^{min/+}$ mice was dramatically higher than that in tumors of $Vhl^{F/F}/Apc^{min/+}$ mice, whereas low-iron diet treatment greatly decreased the number of BrdU positive epithelial cells in the tumor colon tissues of both $Vhl^{F/F}/Apc^{min/+}$ and $Vhl^{\Delta IE}/Apc^{min/+}$ mice (Figure 6B). These results demonstrate that tumoral iron is essential for colon cancer progression and a critical pathway by which HIF-2α signaling contributes to colon tumorigensis.

Discussion

Hypoxia is an adaptive response in many solid tumors. However, its role in tumor development *in vivo* is still not clear. The present study found that the activation of HIF signaling through HIF-2α enhanced colon cancer incidence and progression in the $Apc^{min/+}$ mice. The *Apc* tumor suppressor is a gatekeeper gene mutated in a majority of patients with familial, sporadic, and colitis-associated colon cancer(35–38). However, $Apc^{min/+}$ mice develop mostly small intestinal tumors and colon tumors are observed with low incidence and multiplicity(34). HIF-2α activation in the intestines of $Vhl^{\Delta IE}/Apc^{min/+}$ mice dramatically increased colon tumor multiplicity and incidence. Moreover, at 6 months of age the majority of colon tumors observed were histologically defined as carcinomas, whereas no tumors identified in the $Vhl^{F/F}/Apc^{min/+}$ mice progressed further than adenomas, demonstrating that HIF-2α may be a critical transcription factor involved in colon cancer progression.

Interestingly, small intestinal tumors observed in the $Vhl^{\Delta IE}/Apc^{min/+}$ mice were rare and this decrease in tumorigenesis was independent of HIF-2α expression. Despite the profound decrease in tumorigenesis, no changes in small intestinal proliferation were observed between $Vhl^{\Delta IE}/Apc^{min/+}$ and $Vhl^{F/F}/Apc^{min/+}$ mice (Supplemental Figure 5). Moreover, the $Vhl^{\Delta IE}/Apc^{min/+}$ mice had increased DMT-1 expression in the small intestine, suggesting that decreased small intestinal tumorigenesis by the HIF-2α-independent mechanism is downstream of the iron accumulation effects. HIF-1α was shown to have an antagonistic role in cell growth and VHL has several HIF-independent functions(11, 48–52), and these pathways are currently being assessed in the small intestine. There is some evidence that colon tumors in the $Apc^{min/+}$ do not form because of the large tumor load of the small intestine compromise the mice, therefore the slower forming colon tumors do not develop. However, in the $Vhl^{\Delta IE}/Hif\text{-}2\alpha^{\Delta IE}/Apc^{min/+}$ mice, the decrease in small intestinal tumors, did not lead to a refractory increase in colon tumors. Confirming that the increase in colon tumors in the $Vhl^{\Delta IE}/Apc^{min/+}$ mice is mediated by HIF-2α activation. The $Vhl^{\Delta IE}/Apc^{min/+}$ mice, through HIF-2α-dependent and -independent mechanisms, can recapitulate downstream events following *Apc* mutation that is observed in sporadic, familial, and colitis-associated colon cancer, and is an optimal pre-clinical animal model to study colon cancer.

The mechanisms that decrease small intestinal tumorigenesis are currently not known. However, the increases in colon tumor incidence, multiplicity, and progression in *Vhl*$^{\Delta IE}$/*Apc*$^{min/+}$ mice was completely ablated following double knockout of *Vhl* and *Hif-2α* in the *Apc*$^{min/+}$ background, demonstrating that HIF-2α plays a critical role in the development of colon cancer following *Apc*$^{min/+}$ mutation. Activation of HIF-2α in the intestine increased epithelial cell survival. This was measured using colon organoids that may be in undergoing apoptosis very early following the culture of the colons and using colon cancer-derived cells lines. Therefore, the anoikis detected may not be a physiological response and a more detailed analysis of HIF-2α mediated cell survival is needed. However, the present study clearly demonstrates a role of HIF-2α in tumor proliferation. To understand the mechanisms involved in the increase in colon tumorigenesis, the HIF-2α-dependent gene expression profile was analyzed by the ONCOMINE database(41). The HIF-2α target gene DMT-1 was highly induced in colon adenomas and carcinomas compared to normal colon tissue isolated from patients. DMT-1 is a critical intestinal iron transporter and its overexpression can lead to iron accumulation(45, 46, 53, 54). Iron accumulation is a critical factor in colon carcinogenesis and studies have shown that both body iron stores and dietary iron intake are positively associated with subsequent risk of colon cancer(22). In mouse models of colon cancer, iron-enriched diets increase the development of colon tumors(21). Iron activates free radical formation, which have a pleiotropic effect in carcinogenesis, including increase in cell survival and proliferation, which is consistent with the present study. Together the data suggest that HIF-2α mediated dysregulation of intestinal iron transport is critical for the increase in colon tumors observed in the *Vhl*$^{\Delta IE}$/*Apc*$^{min/+}$ mice. Therefore inhibition of HIF-2α activation in colon tumors may represent a potential strategy for the prevention and treatment of colon cancer. Moreover, our data suggest that iron chelators will be beneficial for patients with colon cancer. It is important to note that HIF-2α activates a large battery of genes in the intestine and its mechanistic role in tumor development is most likely through multiple pathways. However, in the present study we clearly demonstrate that the activation of HIF-2α contributes to the increase in cell proliferation, dysregulation of local iron homeostasis, and eventually an increase in the incidence of colon cancer.

Supplementary Material

Refer to Web version on PubMed Central for supplementary material.

Acknowledgments

We thank Dr. Bishr Omary for providing cleaved K18 antibody. The University of Michigan Cancer Center Microarray Core for Affymetrix gene array services and analysis.

Grant Support

This study was supported by grants to Y.M.S from the National Institutes of Health (CA148828), The University of Michigan Gastrointestinal Peptide Center, and Jeffrey A. Colby Colon Cancer Research and the Tom Liu Memorial Funds of the University of Michigan Comprehensive Cancer Center. F.J.G was supported by the Intramural Research Program of the National Cancer Institute.

Reference

1. Hockel M, Vaupel P. Tumor hypoxia: definitions and current clinical, biologic, and molecular aspects. J Natl Cancer Inst. 2001; 93:266–276. [PubMed: 11181773]
2. Bertout JA, Patel SA, Simon MC. The impact of O2 availability on human cancer. Nat Rev Cancer. 2008; 8:967–975. [PubMed: 18987634]
3. Semenza GL, Wang GL. A nuclear factor induced by hypoxia via de novo protein synthesis binds to the human erythropoietin gene enhancer at a site required for transcriptional activation. Mol Cell Biol. 1992; 12:5447–5454. [PubMed: 1448077]

4. Wang GL, Semenza GL. Characterization of hypoxia-inducible factor 1 and regulation of DNA binding activity by hypoxia. J Biol Chem. 1993; 268:21513–21518. [PubMed: 8408001]
5. Wang GL, Semenza GL. General involvement of hypoxia-inducible factor 1 in transcriptional response to hypoxia. Proc Natl Acad Sci U S A. 1993; 90:4304–4308. [PubMed: 8387214]
6. Ivan M, Kondo K, Yang H, Kim W, Valiando J, Ohh M, et al. HIFalpha targeted for VHL-mediated destruction by proline hydroxylation: implications for O2 sensing. Science. 2001; 292:464–468. [PubMed: 11292862]
7. Jaakkola P, Mole DR, Tian YM, Wilson MI, Gielbert J, Gaskell SJ, et al. Targeting of HIF-alpha to the von Hippel-Lindau ubiquitylation complex by O2-regulated prolyl hydroxylation. Science. 2001; 292:468–472. [PubMed: 11292861]
8. Wang GL, Jiang BH, Rue EA, Semenza GL. Hypoxia-inducible factor 1 is a basic-helix-loop-helix-PAS heterodimer regulated by cellular O2 tension. Proc Natl Acad Sci U S A. 1995; 92:5510–5514. [PubMed: 7539918]
9. Tian H, McKnight SL, Russell DW. Endothelial PAS domain protein 1 (EPAS1), a transcription factor selectively expressed in endothelial cells. Genes Dev. 1997; 11:72–82. [PubMed: 9000051]
10. Loboda A, Jozkowicz A, Dulak J. HIF-1 and HIF-2 transcription factors--similar but not identical. Mol Cells. 2010; 29:435–442. [PubMed: 20396958]
11. Gordan JD, Bertout JA, Hu CJ, Diehl JA, Simon MC. HIF-2alpha promotes hypoxic cell proliferation by enhancing c-myc transcriptional activity. Cancer Cell. 2007; 11:335–347. [PubMed: 17418410]
12. Gordan JD, Lal P, Dondeti VR, Letrero R, Parekh KN, Oquendo CE, et al. HIF-alpha effects on c-Myc distinguish two subtypes of sporadic VHL-deficient clear cell renal carcinoma. Cancer Cell. 2008; 14:435–446. [PubMed: 19061835]
13. Wen W, Ding J, Sun W, Wu K, Ning B, Gong W, et al. Suppression of cyclin D1 by hypoxia-inducible factor-1 via direct mechanism inhibits the proliferation and 5-fluorouracil-induced apoptosis of A549 cells. Cancer Res. 2010; 70:2010–2019. [PubMed: 20179204]
14. Goda N, Ryan HE, Khadivi B, McNulty W, Rickert RC, Johnson RS. Hypoxia-inducible factor 1alpha is essential for cell cycle arrest during hypoxia. Mol Cell Biol. 2003; 23:359–369. [PubMed: 12482987]
15. Koshiji M, Kageyama Y, Pete EA, Horikawa I, Barrett JC, Huang LE. HIF-1alpha induces cell cycle arrest by functionally counteracting Myc. Embo J. 2004; 23:1949–1956. [PubMed: 15071503]
16. Hubbi ME, Luo W, Baek JH, Semenza GL. MCM proteins are negative regulators of hypoxia-inducible factor 1. Mol Cell. 2011; 42:700–712. [PubMed: 21658608]
17. Talks KL, Turley H, Gatter KC, Maxwell PH, Pugh CW, Ratcliffe PJ, et al. The expression and distribution of the hypoxia-inducible factors HIF-1alpha and HIF-2alpha in normal human tissues, cancers, and tumor-associated macrophages. Am J Pathol. 2000; 157:411–421. [PubMed: 10934146]
18. Zhong H, De Marzo AM, Laughner E, Lim M, Hilton DA, Zagzag D, et al. Overexpression of hypoxia-inducible factor 1alpha in common human cancers and their metastases. Cancer Res. 1999; 59:5830–5835. [PubMed: 10582706]
19. Sesink AL, Termont DS, Kleibeuker JH, Van der Meer R. Red meat and colon cancer: the cytotoxic and hyperproliferative effects of dietary heme. Cancer Res. 1999; 59:5704–5709. [PubMed: 10582688]
20. Bastide NM, Pierre FH, Corpet DE. Heme iron from meat and risk of colorectal cancer: a meta-analysis and a review of the mechanisms involved. Cancer Prev Res (Phila). 2011; 4:177–184. [PubMed: 21209396]
21. Siegers CP, Bumann D, Baretton G, Younes M. Dietary iron enhances the tumor rate in dimethylhydrazine-induced colon carcinogenesis in mice. Cancer Lett. 1988; 41:251–256. [PubMed: 3409203]
22. Nelson RL, Davis FG, Sutter E, Sobin LH, Kikendall JW, Bowen P. Body iron stores and risk of colonic neoplasia. J Natl Cancer Inst. 1994; 86:455–460. [PubMed: 8120921]

23. Siegers CP, Bumann D, Trepkau HD, Schadwinkel B, Baretton G. Influence of dietary iron overload on cell proliferation and intestinal tumorigenesis in mice. Cancer Lett. 1992; 65:245–249. [PubMed: 1516040]
24. Nelson RL. Iron and colorectal cancer risk: human studies. Nutr Rev. 2001; 59:140–148. [PubMed: 11396694]
25. Seril DN, Liao J, Ho KL, Warsi A, Yang CS, Yang GY. Dietary iron supplementation enhances DSS-induced colitis and associated colorectal carcinoma development in mice. Dig Dis Sci. 2002; 47:1266–1278. [PubMed: 12064801]
26. Shah YM, Matsubara T, Ito S, Yim SH, Gonzalez FJ. Intestinal hypoxia-inducible transcription factors are essential for iron absorption following iron deficiency. Cell Metab. 2009; 9:152–164. [PubMed: 19147412]
27. Haase VH, Glickman JN, Socolovsky M, Jaenisch R. Vascular tumors in livers with targeted inactivation of the von Hippel-Lindau tumor suppressor. Proc Natl Acad Sci U S A. 2001; 98:1583–1588. [PubMed: 11171994]
28. Taylor M, Qu A, Anderson ER, Matsubara T, Martin A, Gonzalez FJ, et al. Hypoxia-inducible factor-2alpha mediates the adaptive increase of intestinal ferroportin during iron deficiency in mice. Gastroenterology. 2011; 140:2044–2055. [PubMed: 21419768]
29. Xiao Y, Xue X, Wu YF, Xin GZ, Qian Y, Xie TP, et al. beta-Naphthoflavone protects mice from aristolochic acid-I-induced acute kidney injury in a CYP1A dependent mechanism. Acta Pharmacol Sin. 2009; 30:1559–1565. [PubMed: 19890363]
30. Meguro R, Asano Y, Iwatsuki H, Shoumura K. Perfusion-Perls and -Turnbull methods supplemented by DAB intensification for nonheme iron histochemistry: demonstration of the superior sensitivity of the methods in the liver, spleen, and stomach of the rat. Histochem Cell Biol. 2003; 120:73–82. [PubMed: 12802595]
31. Frisch SM, Francis H. Disruption of epithelial cell-matrix interactions induces apoptosis. J Cell Biol. 1994; 124:619–626. [PubMed: 8106557]
32. Folkman J, Moscona A. Role of cell shape in growth control. Nature. 1978; 273:345–349. [PubMed: 661946]
33. Shah YM, Ito S, Morimura K, Chen C, Yim SH, Haase VH, et al. Hypoxia-inducible factor augments experimental colitis through an MIF-dependent inflammatory signaling cascade. Gastroenterology. 2008; 134:2036–2048. e1–e3. 48. [PubMed: 18439915]
34. Su LK, Kinzler KW, Vogelstein B, Preisinger AC, Moser AR, Luongo C, et al. Multiple intestinal neoplasia caused by a mutation in the murine homolog of the APC gene. Science. 1992; 256:668–670. [PubMed: 1350108]
35. Fearnhead NS, Britton MP, Bodmer WF. The ABC of APC. Hum Mol Genet. 2001; 10:721–733. [PubMed: 11257105]
36. Cooper HS, Everley L, Chang WC, Pfeiffer G, Lee B, Murthy S, et al. The role of mutant Apc in the development of dysplasia and cancer in the mouse model of dextran sulfate sodium-induced colitis. Gastroenterology. 2001; 121:1407–1416. [PubMed: 11729120]
37. Pastorelli L, Garg RR, Hoang SB, Spina L, Mattioli B, Scarpa M, et al. Epithelial-derived IL-33 and its receptor ST2 are dysregulated in ulcerative colitis and in experimental Th1/Th2 driven enteritis. Proc Natl Acad Sci U S A. 2010; 107:8017–8022. [PubMed: 20385815]
38. Redston MS, Papadopoulos N, Caldas C, Kinzler KW, Kern SE. Common occurrence of APC and K-ras gene mutations in the spectrum of colitis-associated neoplasias. Gastroenterology. 1995; 108:383–392. [PubMed: 7835579]
39. Jemal A, Siegel R, Ward E, Hao Y, Xu J, Murray T, et al. Cancer statistics, 2008. CA Cancer J Clin. 2008; 58:71–96. [PubMed: 18287387]
40. Vachon PH, Harnois C, Grenier A, Dufour G, Bouchard V, Han J, et al. Differentiation state-selective roles of p38 isoforms in human intestinal epithelial cell anoikis. Gastroenterology. 2002; 123:1980–1991. [PubMed: 12454855]
41. Rhodes DR, Chinnaiyan AM. Integrative analysis of the cancer transcriptome. Nat Genet. 2005; 37(Suppl):S31–S37. [PubMed: 15920528]

42. Zou TT, Selaru FM, Xu Y, Shustova V, Yin J, Mori Y, et al. Application of cDNA microarrays to generate a molecular taxonomy capable of distinguishing between colon cancer and normal colon. Oncogene. 2002; 21:4855–4862. [PubMed: 12101425]
43. Skrzypczak M, Goryca K, Rubel T, Paziewska A, Mikula M, Jarosz D, et al. Modeling oncogenic signaling in colon tumors by multidirectional analyses of microarray data directed for maximization of analytical reliability. PLoS One. 2010; 5
44. Sabates-Bellver J, Van der Flier LG, de Palo M, Cattaneo E, Maake C, Rehrauer H, et al. Transcriptome profile of human colorectal adenomas. Mol Cancer Res. 2007; 5:1263–1275. [PubMed: 18171984]
45. Gunshin H, Mackenzie B, Berger UV, Gunshin Y, Romero MF, Boron WF, et al. Cloning and characterization of a mammalian proton-coupled metal-ion transporter. Nature. 1997; 388:482–488. [PubMed: 9242408]
46. Fleming MD, Trenor CC 3rd, Su MA, Foernzler D, Beier DR, Dietrich WF, et al. Microcytic anaemia mice have a mutation in Nramp2, a candidate iron transporter gene. Nat Genet. 1997; 16:383–386. [PubMed: 9241278]
47. Canonne-Hergaux F, Gruenheid S, Ponka P, Gros P. Cellular and subcellular localization of the Nramp2 iron transporter in the intestinal brush border and regulation by dietary iron. Blood. 1999; 93:4406–4417. [PubMed: 10361139]
48. Kaelin WG Jr. The von Hippel-Lindau tumour suppressor protein: O2 sensing and cancer. Nat Rev Cancer. 2008; 8:865–873. [PubMed: 18923434]
49. Young AP, Schlisio S, Minamishima YA, Zhang Q, Li L, Grisanzio C, et al. VHL loss actuates a HIF-independent senescence programme mediated by Rb and p400. Nat Cell Biol. 2008; 10:361–369. [PubMed: 18297059]
50. Kurban G, Hudon V, Duplan E, Ohh M, Pause A. Characterization of a von Hippel Lindau pathway involved in extracellular matrix remodeling, cell invasion, and angiogenesis. Cancer Res. 2006; 66:1313–1319. [PubMed: 16452184]
51. Zhou MI, Wang H, Ross JJ, Kuzmin I, Xu C, Cohen HT. The von Hippel-Lindau tumor suppressor stabilizes novel plant homeodomain protein Jade-1. J Biol Chem. 2002; 277:39887–39898. [PubMed: 12169691]
52. Russell RC, Sufan RI, Zhou B, Heir P, Bunda S, Sybingco SS, et al. Loss of JAK2 regulation via a heterodimeric VHL-SOCS1 E3 ubiquitin ligase underlies Chuvash polycythemia. Nat Med. 2011; 17:845–853. [PubMed: 21685897]
53. Foot NJ, Leong YA, Dorstyn LE, Dalton HE, Ho K, Zhao L, et al. Ndfip1-deficient mice have impaired DMT1 regulation and iron homeostasis. Blood. 2011; 117:638–646. [PubMed: 20959604]
54. Foot NJ, Dalton HE, Shearwin-Whyatt LM, Dorstyn L, Tan SS, Yang B, et al. Regulation of the divalent metal ion transporter DMT1 and iron homeostasis by a ubiquitin-dependent mechanism involving Ndfips and WWP2. Blood. 2008; 112:4268–4275. [PubMed: 18776082]

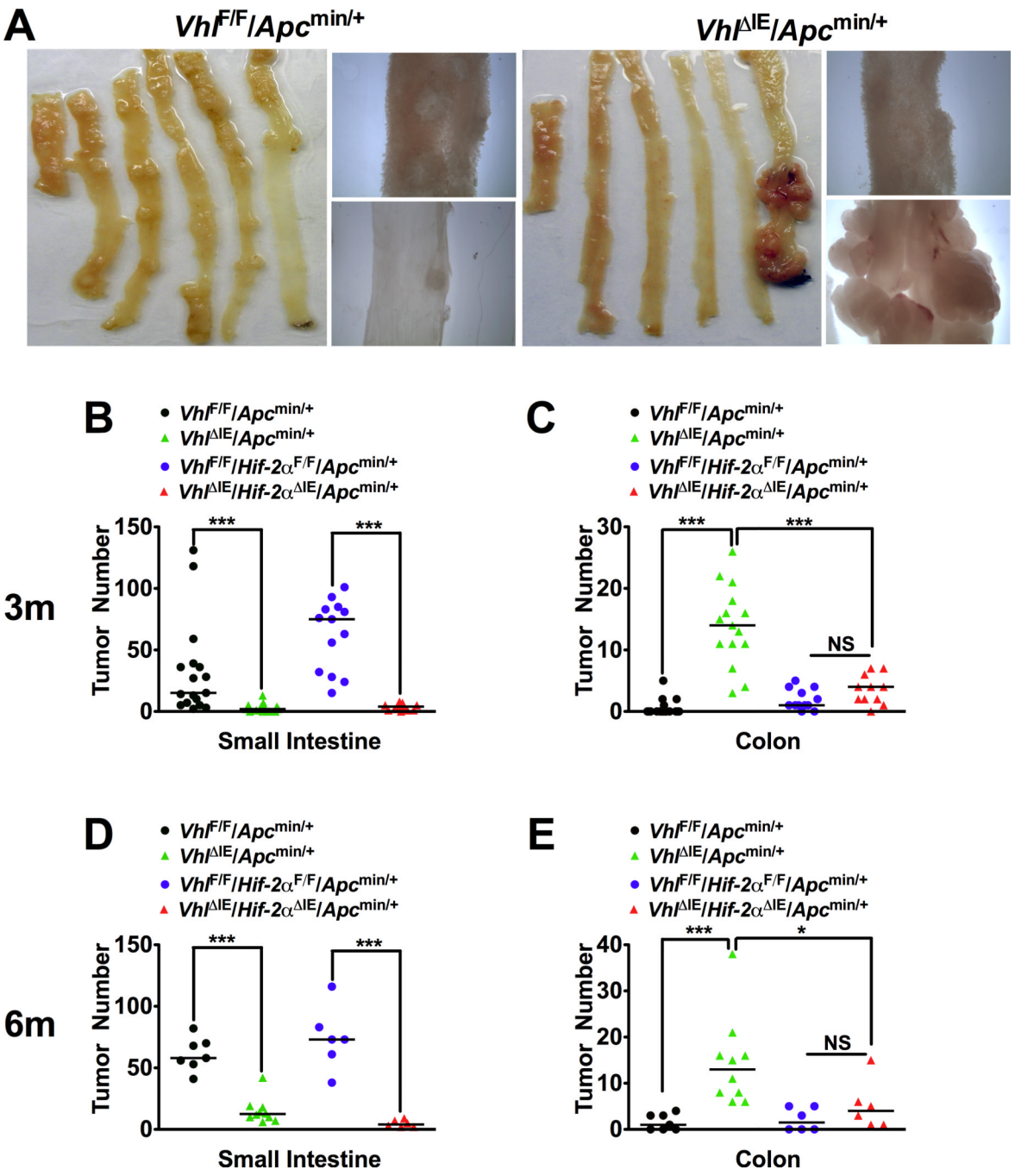

Figure 1. HIF-2α modulates intestinal tumorigenesis in *Apc*$^{min/+}$ mice

(**A**) Representative colons from *Vhl*$^{F/F}$/*Apc*$^{min/+}$ (n=24) and *Vhl*$^{\Delta IE}$/*Apc*$^{min/+}$ mice (n=25). Tumor counting in the small intestine (**B**) and colon (**C**) from 3-month-old *Vhl*$^{F/F}$/*Apc*$^{min/+}$ (n=17), *Vhl*$^{\Delta IE}$/*Apc*$^{min/+}$ (n=15), *Vhl*$^{F/F}$/*Hif-2α*$^{F/F}$/*Apc*$^{min/+}$ (n=13) and *Vhl*$^{\Delta IE}$/*Hif-2α*$^{\Delta IE}$/*Apc*$^{min/+}$ mice (n=11). Tumor counting in the small intestine (**D**) and colon (**E**) from 6-month-old *Vhl*$^{F/F}$/*Apc*$^{min/+}$ (n=7), *Vhl*$^{\Delta IE}$/*Apc*$^{min/+}$ (n=10), *Vhl*$^{F/F}$/*Hif-2α*$^{F/F}$/*Apc*$^{min/+}$ (n=6), and *Vhl*$^{\Delta IE}$/*Hif-2α*$^{\Delta IE}$/*Apc*$^{min/+}$ mice (n=6). *p<0.05 and ***p<0.001; NS, not significant.

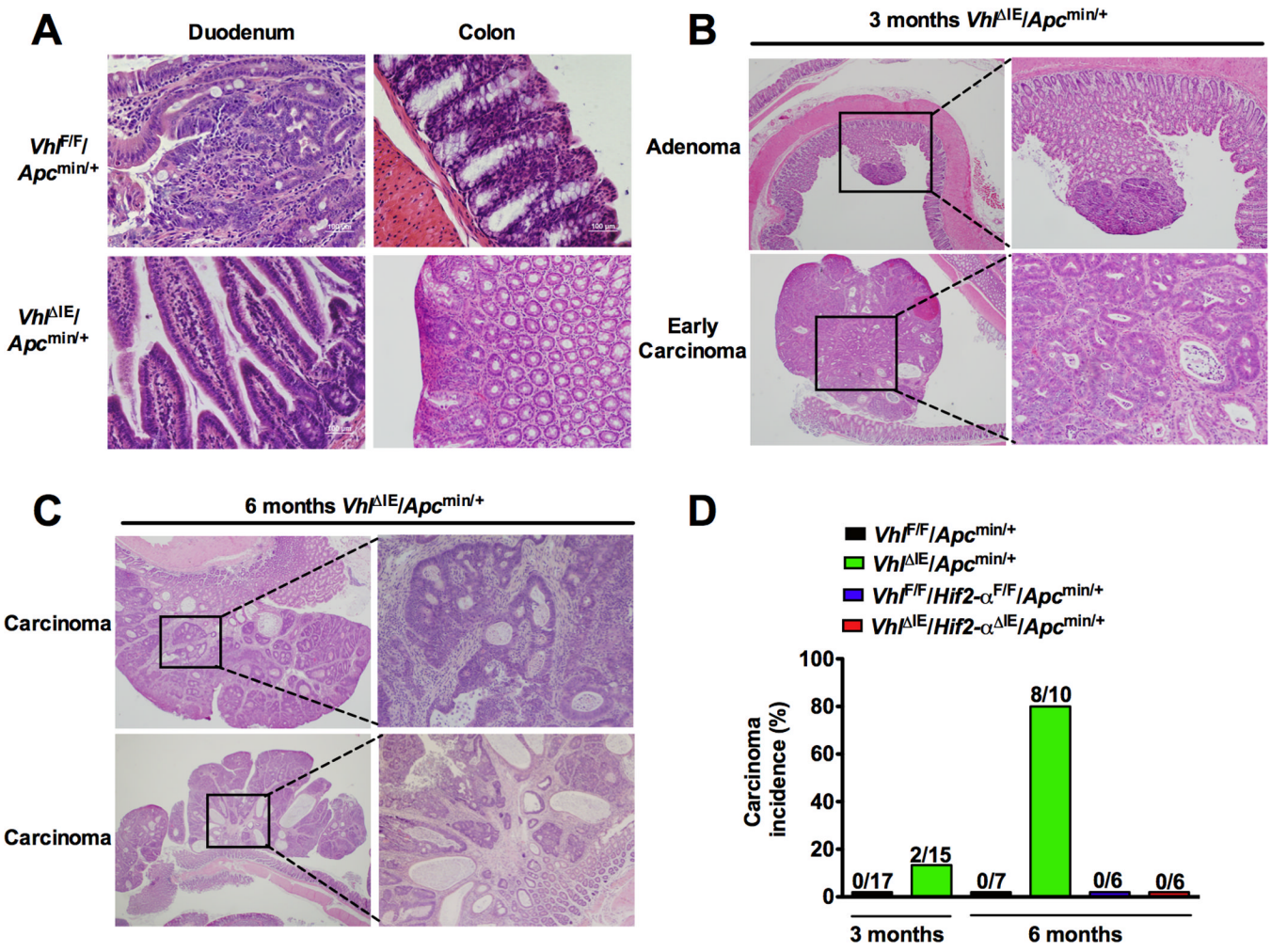

Figure 2. HIF-2α promotes carcinoma formation in *Apc*$^{min/+}$ mice

(**A**) H & E staining of representative duodenum and colon from 3-month-old *Vhl*$^{F/F}$/*Apc*$^{min/+}$ and *Vhl*$^{\Delta IE}$/*Apc*$^{min/+}$ mice. (**B**) H & E staining of representative colon from 3-month-old Vhl$^{\Delta IE}$/Apc$^{min/+}$ mice with an adenoma and progression to early stage carcinoma. (**C**) H & E staining of representative colon carcinoma from 6-month-old *Vhl*$^{\Delta IE}$/*Apc*$^{min/+}$ mice. (**D**) Incidence of carcinoma in 3- and 6-month *Vhl*$^{F/F}$/*Apc*$^{min/+}$, *Vhl*$^{\Delta IE}$/*Apc*$^{min/+}$, *Vhl*$^{F/F}$/*Hif-2α*$^{F/F}$/*Apc*$^{min/+}$, and *Vhl*$^{\Delta IE}$/*Hif-2α*$^{\Delta IE}$/*Apc*$^{min/+}$ mice.

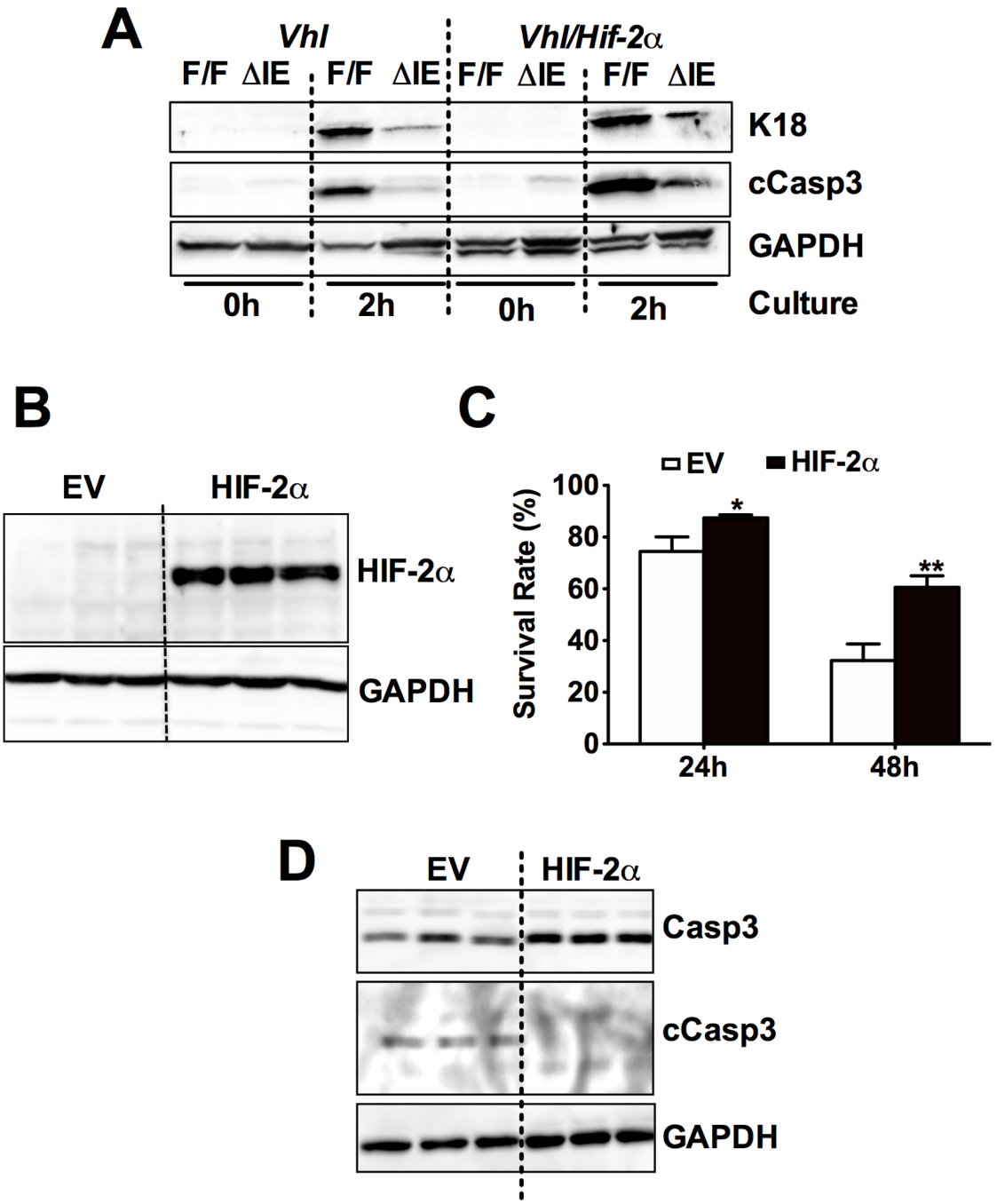

Figure 3. HIF-2α increases cell survival in the colon

(**A**) Western blot for cleaved caspase 3 (cCasp 3), cleaved keratin 18 (K18), and GAPDH in colon organoid cultures from $Vhl^{F/F}$, $Vhl^{\Delta IE}$, $Vhl^{F/F}/Hif\text{-}2\alpha^{F/F}$, and $Vhl^{\Delta IE}/Hif\text{-}2\alpha^{\Delta IE}$ mice incubated for 0 h or 2 h at 37 °C. (**B**) Western Blot analysis for HIF-2α and GAPDH from HCT116 stably transfected with empty vector (EV) or HIF-2α plasmid. (**C**) Cell survival rate of HCT116 cells stably transfected with EV or HIF-2α plasmid in an anoikis-induced apoptosis assay. Survival rates were compared to uncoated control plates. Each bar represents the mean value ± S.D. (n=3). *p<0.05 and **p<0.01, versus EV. (**D**) Western

Blot analysis for cCasp3, total caspase 3 (Casp3), and GAPDH from HCT116 cells stably transfected with EV or HIF-2α plasmid 24 h following induction of anoikis.

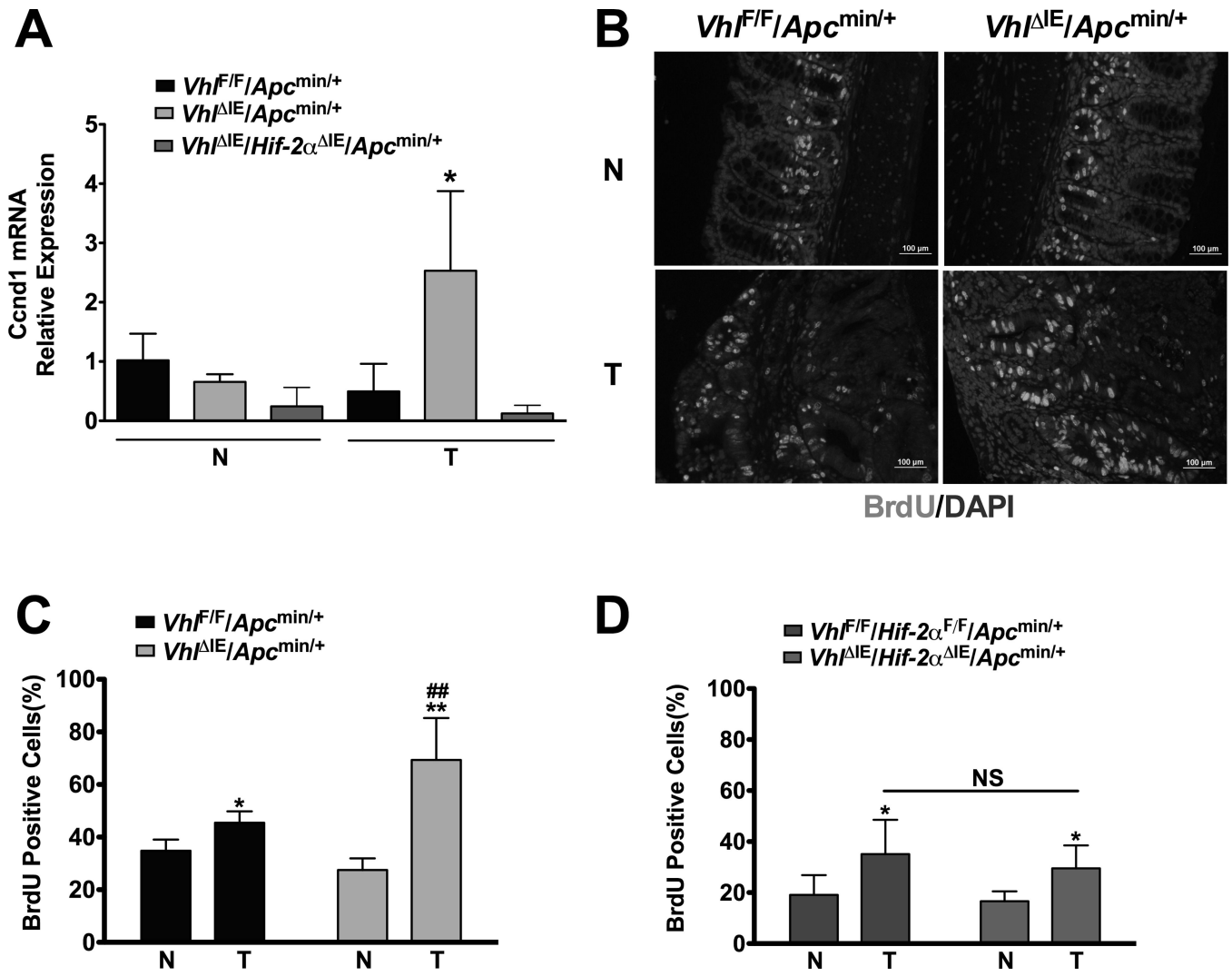

Figure 4. HIF-2α increases cell proliferation in the colon tumors

(**A**) qPCR analysis of cyclin D1 (Ccnd1) in normal and tumor colon tissues from *Vhl*$^{F/F}$/Apc$^{min/+}$, *Vhl*$^{\Delta IE}$/Apc$^{min/+}$, and *Vhl*$^{\Delta IE}$/*Hif-2α*$^{\Delta IE}$/*Apc*$^{min/+}$ mice. Each bar represents the mean value ± S.D. (n=4). Expression was normalized to β-actin. (**B**) BrdU staining and **(C)** quantification in normal and tumor colon tissues from 6-month-old *Vhl*$^{F/F}$/Apc$^{min/+}$ and *Vhl*$^{\Delta IE}$/Apc$^{min/+}$ mice 2-hour following 100 mg/kg BrdU intraperitoneal injection. Each bar represents the mean value ± S.D. (n=4). **(D)** BrdU staining and quantification in normal and tumor colon tissues from *Vhl*$^{F/F}$/*Hif-2α*$^{F/F}$/*Apc*$^{min/+}$ and *Vhl*$^{\Delta IE}$/*Hif-2α*$^{\Delta IE}$/*Apc*$^{min/+}$ mice 2-hour following 100 mg/kg BrdU intraperitoneal injection. N, normal tissue; T, tumor tissue; NS, not significant; *p<0.05, **p<0.01 versus normal tissue; ## p<0.01 versus *Vhl*$^{F/F}$/Apc$^{min/+}$ mice. Each bar represents the mean value ± S.D. (n=4).

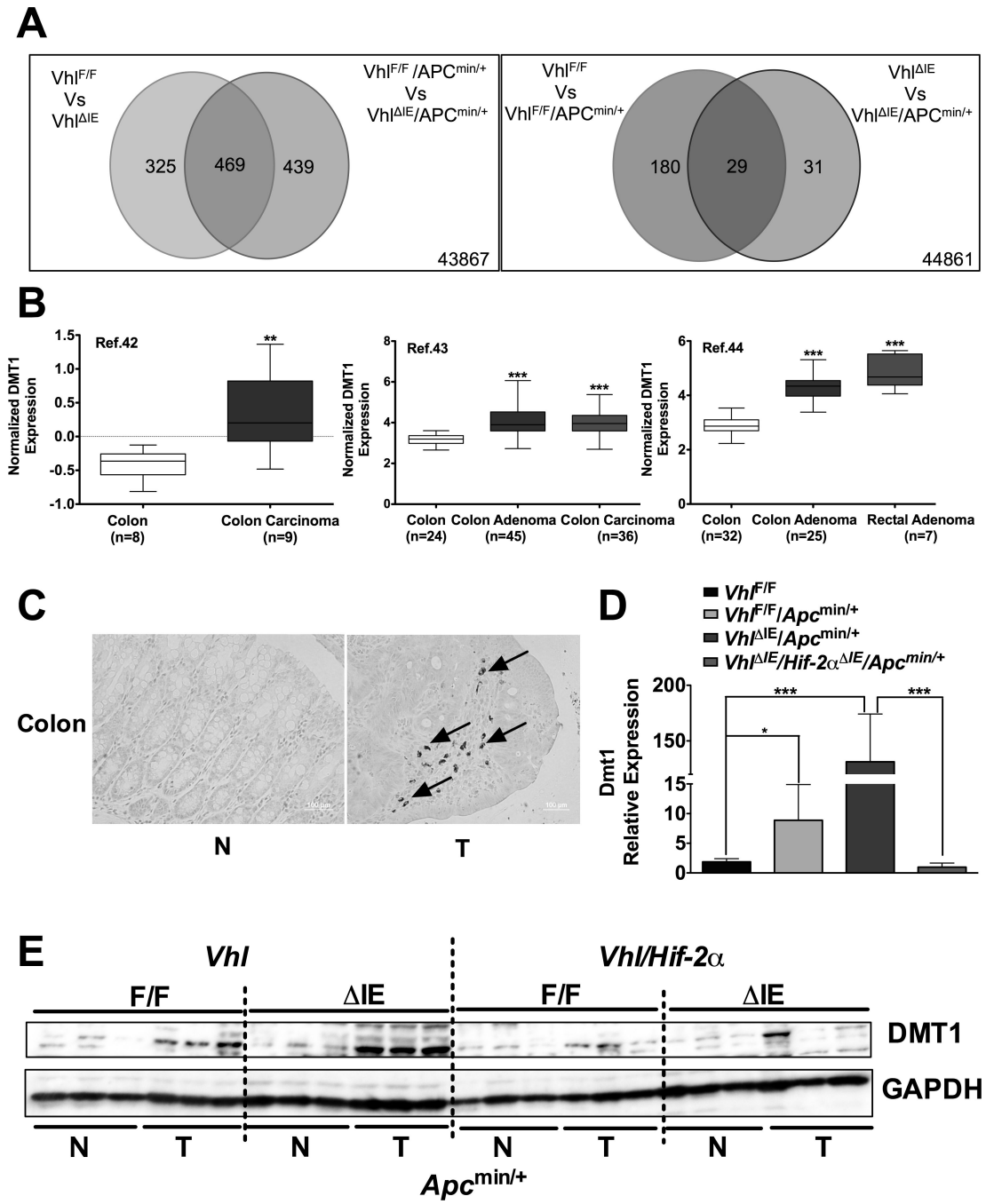

Figure 5. DMT-1 expression in colon tumors

(**A**) Global gene expression profiling in colon RNAs isolated from 5-week-old *Vhl*$^{F/F}$ (n=4), *Vhl*$^{F/F}$/Apc$^{min/+}$(n=3), *Vhl*$^{\Delta IE}$ (n=3) and *Vhl*$^{\Delta IE}$/*Apc*$^{min/+}$ mice (n=5). (**B**) DMT1 gene expression levels in three independent human colon cancer studies were analyzed using ONCOMINE. **p<0.01,***p<0.001 versus normal colon tissue. (**C**) Enhanced Prussian blue staining for iron in normal colon and colon cancer tissue. Arrows indicate iron staining. (**D**) qPCR analysis of Dmt1 in colon epithelial cells from *Vhl*$^{F/F}$ (n=6), *Vhl*$^{F/F}$/Apc$^{min/+}$ (n=5), *Vhl*$^{\Delta IE}$/Apc$^{min/+}$ (n=5) and *Vhl*$^{\Delta IE}$/*Hif-2α*$^{\Delta IE}$/Apc$^{min/+}$ mice (n=3). Expression was normalized to β-actin. *p<0.05,***p<0.001 (**E**) Western Blot analysis for DMT-1 and

GAPDH from normal and tumor colon tissues of 3-month-old $Vhl^{F/F}$/$Apc^{min/+}$, $Vhl^{\Delta IE}$/$Apc^{min/+}$, $Vhl^{F/F}$/*Hif-2α*$^{F/F}$/$Apc^{min/+}$ and $Vhl^{\Delta IE}$/*Hif-2α*$^{\Delta IE}$/$Apc^{min/+}$ mice. N, normal tissue; T, tumor tissue.

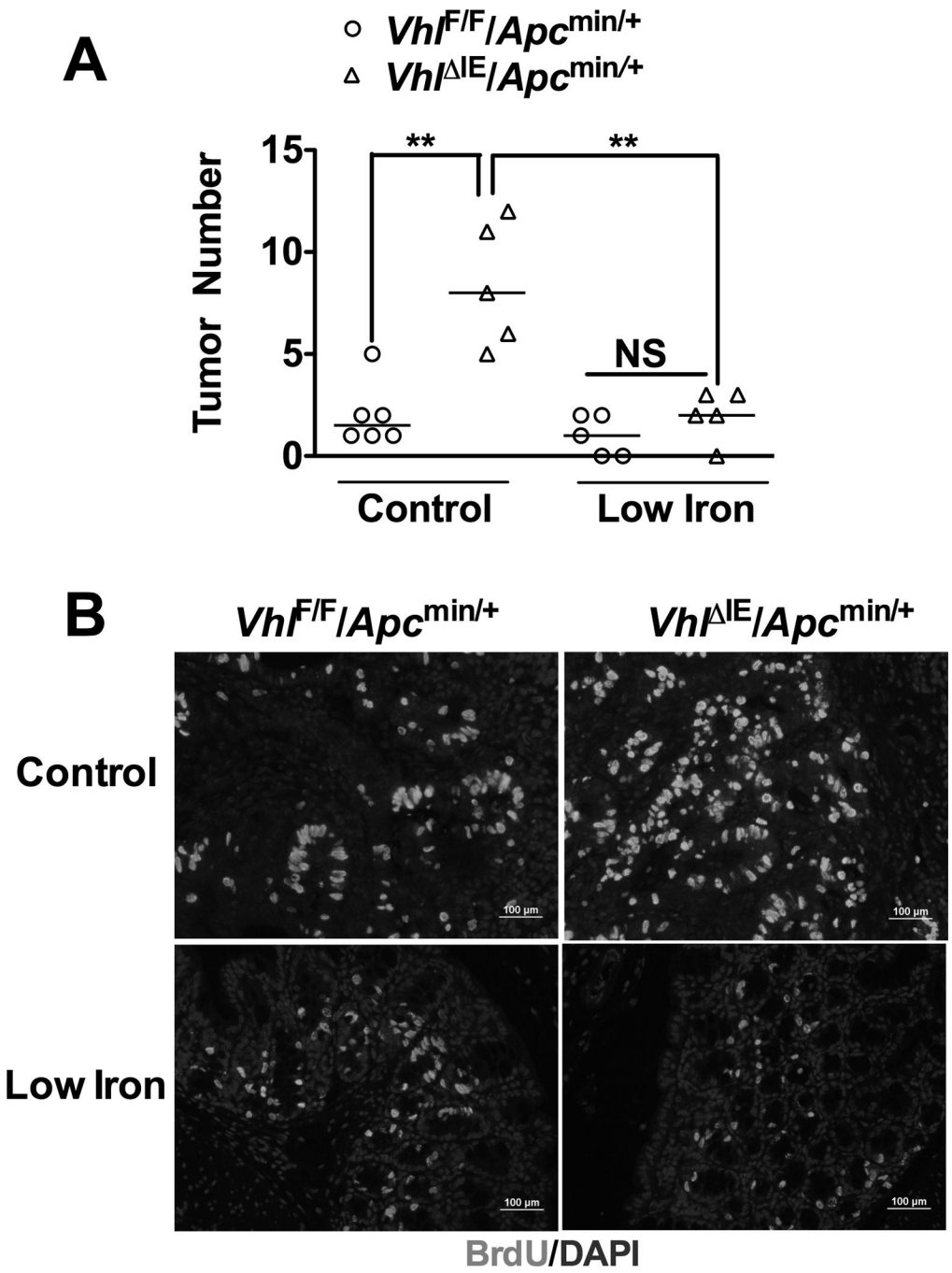

Figure 6. Low-iron diet decreases HIF-2α-mediated intestinal tumorigenesis and cellular proliferation

(**A**) Tumor numbers in the colon from $Vhl^{F/F}/Apc^{min/+}$ (n=11), and $Vhl^{\Delta IE}/Apc^{min/+}$ mice (n=10) treated with control or low-iron diet for 2 months. **p < 0.01; NS, not significant. (**B**) BrdU staining of colon tumors from $Vhl^{F/F}/Apc^{min/+}$ and $Vhl^{\Delta IE}/Apc^{min/+}$ mice treated with control or low-iron diet for 2 months.